Measurement of Flame Frequency Response Functions in a Low-Swirl Flame under Exhaust Gas Recirculation Conditions

Joseph Ranalli[1] and Don Ferguson[2]
National Energy Technology Laboratory, Morgantown, WV 26507

Flame transfer functions provide a useful framework for evaluation of flame dynamics, which play a significant role in the occurrence of thermoacoustic instabilities. Measurements of flame transfer functions were made in a low-swirl injector stabilized flame, and attention was paid to the effects of CO2 and N2 dilution, as a simulation of Exhaust Gas Recirculation conditions. The characteristics of the flame transfer function for the low-swirl injector were observed to be similar to those for more traditional swirl-stabilized flame geometries. The flame transfer function exhibited decreasing gain with increasing frequency and showed evidence of interference of convective disturbances leading to notch features in the transfer function magnitude. The importance of convective disturbances was further supported by the predominant delay characteristic observed in the transfer function phase. Dilution was observed to produce essentially the same effects on the flame transfer function as changes in the equivalence ratio.

I. Introduction

GAS turbine combustion designs face many environmental constraints. Recent pressure has been placed on designs by the potential for regulation of greenhouse gas emissions, including carbon dioxide (CO_2), prompting the need for combustion strategies which may make separation of carbon possible. One proposed "near-term" solution has been the use of Exhaust Gas Recirculation (EGR), which can increase the concentration of CO_2 in the turbine exhaust stream, making post-combustion carbon capture more efficient[1]. The effects of EGR on the combustion process are not well known, but the variation introduced in reactant composition may be expected to include additional factor leading to problematic combustion events such as blowoff and thermoacoustic instabilities. This study aims to address this gap in part by measuring impacts of EGR on these thermoacoustic instabilities in a low-swirl injection (LSI) geometry.

One possible mechanism for thermoacoustic instabilities is coupling between the acoustic velocity and the flame heat release rate. For complete combustion, energy is released by the flame in proportion to the mass flow rate of reactants, which fluctuates due to the acoustics. Acoustic fluctuations are further driven by the heat release rate variations of the flame, resulting in a closed-loop feedback scenario. Dynamic phenomena such as thermoacoustic instabilities lend themselves to study through system models, such as that shown in Fig. 1. The flame dynamics and the system acoustics may be represented by a pair of independent transfer functions (H_f and H_a respectively). These transfer functions describe the frequency dependent response of the flame and acoustics to perturbations, and allow further insight into the physics governing these responses.

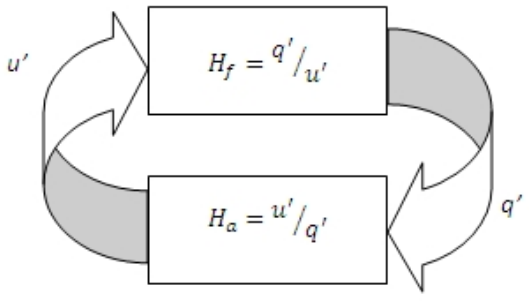

Fig. 1 - Sketch of closed-loop coupling process responsible for thermoacoustic instabilities. q' represents oscillations in the flame heat release rate and u' represents the acoustic velocity.

Complete description of the behavior of the combustor relative to thermoacoustic instabilities requires knowledge

[1] Postdoctoral Research Associate, Member AIAA, joseph.ranalli@or.netl.doe.gov
[2] Research Engineer, Member AIAA, donald.ferguson@netl.doe.gov

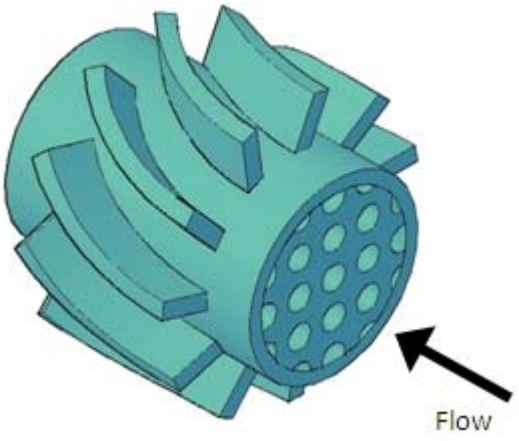

Fig. 2 - CAD drawing of the low-swirl injector used in this study. The arrow indicates the flow direction.

of both the flame and acoustic transfer functions in this system realization. While determination of the acoustic transfer function is not trivial, the techniques for obtaining it are well established. The acoustic transfer function may be measured experimentally or determined from known modeling techniques, e.g. finite element methods. The details of the flame transfer function, however, are still an area of active research and may be further influenced by the variable composition encountered with EGR.

II. Background

While significant attention has been paid to flame dynamics in the literature[2-10], few studies have attempted to characterize the flame dynamics for a flame stabilized using a low-swirl injector. The low-swirl injector used in this study is based on that designed by Cheng[11,12]. Unlike typical "high-swirl" geometries which usually consist of swirling flow around a solid centerbody, the LSI consists of an open central grid surrounded by a set of swirl vanes (see Fig. 2). This configuration generates an undisturbed central flow region where the flame is stabilized by direct propagation into the flow, with an outer swirling flow region where shear effects become important.

Previous work in characterization of LSI impacts on instabilities have focused on the Rayleigh Index, a quantity describing essentially the phasing of the thermoacoustic coupling. Kang *et al.*[13] made measurements of the spatially resolved Rayleigh Index in forced flames for a low-swirl configuration and found a relationship between instabilities and toroidal structures in the shear mixing region near the flame boundary. They also made measurements of a flame transfer function between heat release rate and pressure disturbances. Yilnaz et. al. found similar results in the Rayleigh Index distribution including the effects of Hydrogen addition[14]. With regard to EGR, prior study by Ferguson *et al*[15] has considered the impact of EGR on instabilities in a "high-swirl" geometry, who note the importance of convective delay in the unstable amplitude.

Generally speaking, typical swirl-stabilized flames have been observed to exhibit behavior similar to that expected from a low-pass filter[4,3]; a response in the flame heat release rate occurs at low frequencies of excitation, with the amplitude of the response dying off at increasing frequency. The flame transfer function phase is known to exhibit delay, associated with a non-uniform spatial velocity disturbance, such as vortices that convect through the flame[16,17]. Interference effects associated with this convective behavior are observed to also play a significant role[16], and can be seen quite clearly in the experiments of Palies *et al*[7]. As such, it is often convenient to describe the flame dynamics in terms of Strouhal number (non-dimensional frequency) based on these convective phenomena. In this case Strouhal number is defined as follows:

$$St = \frac{f \cdot x_c}{u_c} \tag{1}$$

The Strouhal number may be thought of as the ratio between the time taken for a disturbance to convect along a characteristic length x_c, at a mean convective velocity u_c, and the period of oscillation $1/f$. This results in the occurrence of interference-like phenomena which determine the flame dynamics. The characteristic length is often based on the distance from the dump plane to the location of the flame center-of-mass, or the total flame length measured from the dump plane[4]. These measures are intuitive for these typical flames, which stabilize on a centerbody. The lifted aerodynamic stabilization scheme of the LSI may make determination of the suitable characteristic length somewhat less certain.

III. Experimental Methodology

This study used a laboratory scale atmospheric dump combustor. A sketch of the combustor setup is shown in Fig. 3. The inlet nozzle was a 21.6 mm diameter stainless steel tube with various access points along the length. A low-swirl injector was used for flame stabilization. The downstream edge of the LSI body was located at a distance of 29.5 mm from the end of the nozzle. The combustion section was a 79 mm diameter, 203mm long quartz tube to

provide access for optical diagnostics. The tube was "short" to prevent self-excited instabilities from naturally occurring, allowing the open-loop response to be measured.

Measurements of the flame transfer function have previously been performed in the past using an open-loop technique in which the flame is allowed to operate under stable conditions and a velocity excitation is deliberately introduced using a loudspeaker or siren[2-4,7,18]. The velocity excitation and heat release rate response can then be measured directly via a variety of diagnostic techniques. In order to provide sufficient coherence between the velocity input and the heat release rate output, the transfer function can be constructed from a series of sine dwell excitations.

For this study, a speaker at the base of the combustor was used to provide the velocity excitation. The speaker amplitude was varied to provide continued coherence between the input and output with variations in the nozzle acoustics. The amplitudes used were tested to ensure that the response measured remained linear (i.e. the transfer function is unchanged with excitation amplitude). The velocity was measured directly upstream of the swirler using a hotwire anemometer inserted through a port in the nozzle. The flame heat release rate (the output of the measurement) was characterized using a global measurement of the OH* radical chemiluminescence[19]. The OH* chemiluminescence measurement was made using a Photomultiplier Tube (PMT) filtered around the 308nm OH* emission. Both the velocity and the heat release rate measurements were normalized to their mean values, giving a normalized magnitude for the flame transfer function. In addition, spatially resolved images of the time averaged (i.e. steady) flame chemiluminescence were acquired using an intensified CCD (ICCD) camera, filtered in the same way as the OH* measurement PMT.

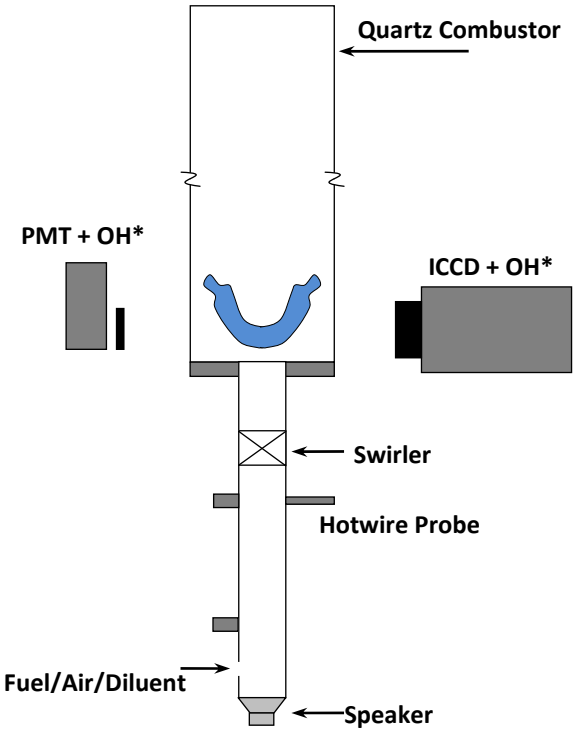

Fig. 3 - Cartoon of the experimental apparatus.

The fuel used in this study was methane with varying levels of nitrogen and carbon dioxide as diluents, to simulate exhaust gas recirculation conditions. A variety of operating conditions with varying flow rate, equivalence ratio and diluent concentration were tested. Fuel, air and diluent were metered using a set of mass flow controllers located upstream of the combustor and were well mixed prior to injection. Dilution levels are reported as a percentage of the total volumetric flow rate. In the case of N2 dilution, the stated dilution percentage represents only the additional N2 added to the flow and excludes the amount of nitrogen already present with the reactant air flow. A choke plate was used to acoustically decouple the mixing section from the rest of the combustor, preventing the occurrence of equivalence ratio or diluent concentration oscillations.

Nondimensionalization of the frequency via the Strouhal number requires a characteristic length and velocity. The velocity used in nondimensionalization was calculated as the mean nozzle velocity based on the flow rate and area of the nozzle tube (21.6 mm diameter), and therefore does not necessarily indicate the exact local convective velocity, but should maintain a proportional relationship with the convective velocity. For lifted flame geometries, several different characteristic lengths may seem like reasonable choices depending on the physics expected. In this case, the characteristic length used was the axial flame length, calculated as the axial distance from the upstream lifted edge of the flame to its furthest downstream edge. The motivation for this particular choice of characteristic length is the idea that flame dynamics result from spatial interference of convected disturbances within the flame[7]. While we believe that this characteristic length is a good choice for the physics of the flame dynamics of the LSI, it was found that several potential characteristic lengths (flame length, distance from dump plane to center of mass, distance from lifted edge to center of mass) all are approximately proportional, implying that each would result in a similarly successful nondimensionalization of the results, though each describes a different physical mechanism.

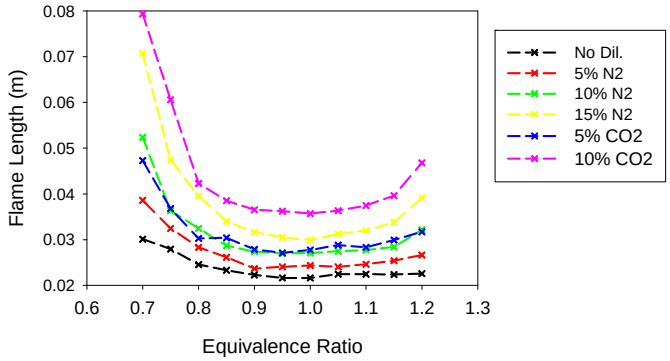

Fig. 4 - Flame Length as a function of equivalence ratio and dilution level. Flow rate is fixed at 100 SLPM. Diluent levels are a percent of the total flow.

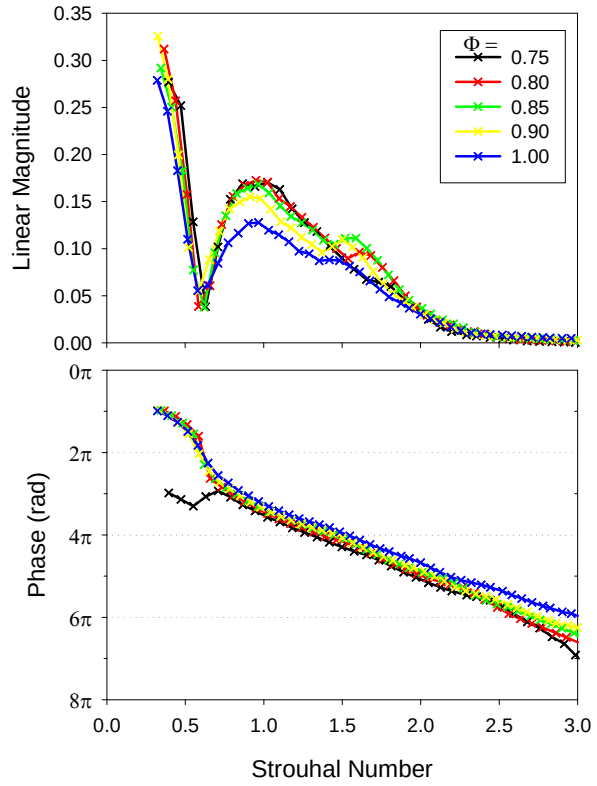

Fig. 5- Measured Flame Transfer Functions as a function of Strouhal Number. Operating condition is methane at

The upstream and downstream flame edges used in the length calculation were identified by thresholding of the steady OH* chemiluminescence images using levels determined algorithmically by the MATLAB Image Processing Toolbox GRAYTHRESH routine. An image of a ruler was used to obtain a calibration for the camera resolution, which was found to be 94 μm per pixel. The steady flame lengths as a function of operating condition are shown in Fig. 4. It is interesting to note that the variations in flame length with respect to equivalence ratio are less significant than those observed for a high-swirl flame in previous studies of this combustor[15]. We believe that this results from the aerodynamic stabilization mechanism of the LSI.

IV. Results & Discussion

The normalized flame transfer function for each of the tested operating cases is shown in Fig. 5. The response is similar in character to that seen for high-swirl flames stabilized with a centerbody[3,4,7] and for laminar flames[2]. The magnitude shows a low-pass filter type response, rolling off with increasing Strouhal number. The total decrease in magnitude agrees with values found in literature for high-swirl configurations. The fact that the phase is predominantly linear is indicative of the important role of convective delay in the dynamics. The extent of the delay can be computed from the slope of the phase curves. Based on the physical offset used in calculating the Strouhal number, the delay for these measurements corresponds with convection along the entire axial flame length at approximately 1.3 times the mean jet velocity.

Another interesting feature of the response is the "notch" observed near a Strouhal number of 0.5. This result mirrors the high-swirl dynamic behavior described by Palies *et al*[7], who also observed a notch around a Strouhal number of 0.5 and used phase-locked flame images to identify out-of-phase oscillations in upstream and downstream regions in the flame as the cause of this notch. Based on this physical description, the notch can be said to occur due to the nature of the convected structures that cause the heat release response. As Strouhal number (i.e. frequency) increases, the wavelength of the spatial perturbations decreases. As this wavelength varies, superimposition of the convective disturbance field[13] with the flame heat release region results in destructive interference (i.e. reductions in global response magnitude). A phase shift of 180° occurs in association with this feature. The difference in direction of the phase shift may be attributed to the shape of the flame heat release profile. Generally, the exact Strouhal Number at which this interference occurs may be influenced by the actual convective velocity field and the shape of the axial heat release profile. However, as long as the characteristic scales being used to represent the velocity and heat release shape are proportional to the actual values, data would be expected to collapse with Strouhal number as seen in the figure.

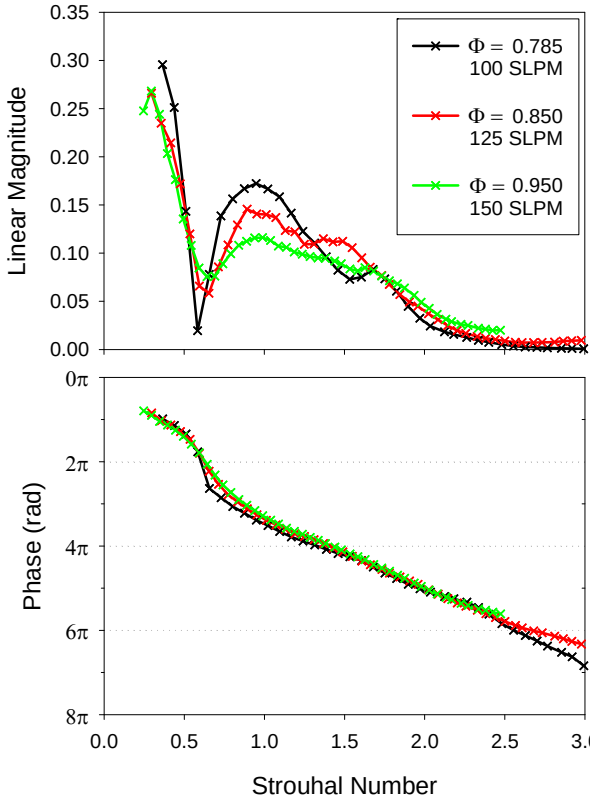

Fig. 6 - Flame transfer functions for methane with varying flow rate with no dilution. Flame length held approximately constant.

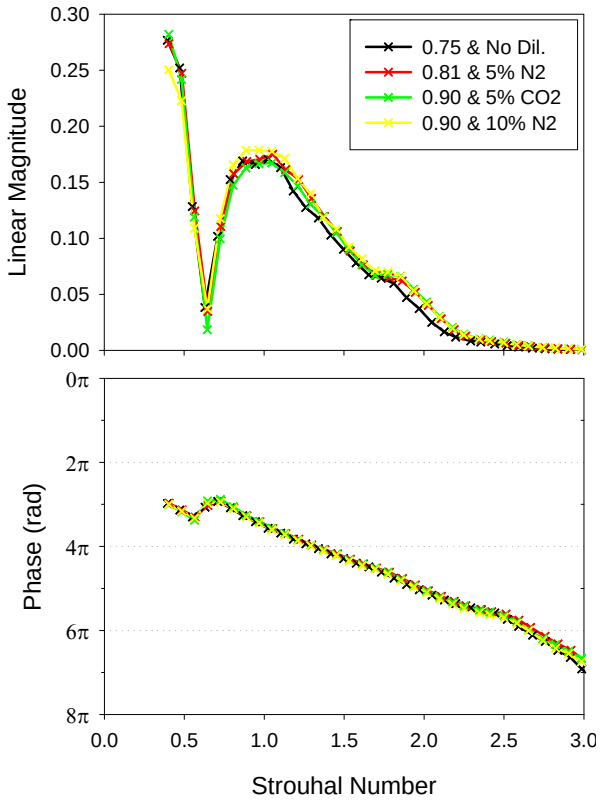

Fig. 7 - Flame Transfer Functions for methane at 100 SLPM with varying levels of dilution. Diluent levels are cited as a percent of the total flow. Flame length held approximately constant.

Additional flame transfer functions were measured with varying flow rate and diluent composition. These results are presented in Fig. 6 and Fig. 7 respectively. In each of these cases, the length of the flame was held approximately constant while the other parameters were varied. The transfer functions for variations in flow rate show variability in the apparent damping of the notch feature discussed previously, though the Strouhal number at which the notch occurs remains relatively constant. In this case increases in the flow rate result in decreases in the severity of the notch. That is, the notch becomes less sharp and the deviation from the overall amplitude trend is reduced. Preliminary modeling efforts suggest that this behavior may be due to variations in the shape of the heat release distribution despite the constant characteristic length.

The results for variation in diluent (Fig. 7) show that at a fixed flow rate, dilution does not introduce new dynamic behaviors. Rather, as long as the flame length is maintained, the response is preserved. In this way, dilution can be said to affect dynamics similarly to changes in equivalence ratio. This is especially significant to considering the effect of EGR on flame dynamics. Generally speaking, increased dilution results in longer flames, with CO2 having a more significant effect than N2 (see Fig. 4). This, just like a shift toward leaner equivalence ratios, corresponds with the flame transfer function features shifting to lower frequencies. Given that the flame length and flame temperature are semi-independent, this fact provides a situation in which dilution could possibly be used in the control of instabilities, allowing different flame lengths (and therefore dynamics) to be achieved at a given flame temperature.

V. Conclusions

The significance of these results is that due to their materially similar flame transfer function, low-swirl injectors would be expected to behave similarly to high-swirl injectors with respect to the occurrence of system instabilities. This result shows that the low-swirl flame does not react to velocity perturbations simply by moving with the flow. Rather, like high-swirl flames, the aerodynamic stabilization mechanism still produces convective disturbances which interact with the flame in a spatially distributed manner. The velocity and heat release rate pass in and out of

phase with respect to frequency due to the delay. Thus, frequencies where self-excitation may occur are likely to depend heavily on this delay, as determined from the flame length and convective velocity. Increases in delay (due to either longer flames, or reduced velocities) would have a tendency to shift in-phase coupling to lower frequencies with the opposite true for decreases in delay.

The flame length excluding the lifting distance was used as a governing characteristic length, corresponding to the physical notion that the convective perturbations arise upon interaction with the flame rather than at the dump plane. However, the fact that several of the other sensible characteristic length scales were approximately proportional to the flame length, it is difficult to be specific about the origin of the convective disturbances leading to the flame response. While the low-swirl flame may be expected to respond similarly to a high-swirl flame in general terms, it is also true that the low-swirl flame was observed to have less significant variations in flame length relative to changes in operating condition. This suggests that there would be less variation in the dynamic response over the operating range and hence, less likelihood to encounter instabilities if beginning from a stable operating condition.

The presence of diluents in the flame was not observed to have a novel impact on the dynamics. The effect of dilution on the dynamics may be characterized in the same way as changes in equivalence ratio and other operating parameters. Existing strategies for predicting and modeling the flame dynamics should continue to apply in the presence of dilution. Analyzing the effect of dilution then becomes one of identifying the ways in which the distribution of the heat release rate is changed with the variable reactant composition.

Acknowledgments

The support of the U.S. DOE Turbines program is gratefully acknowledged. J. Ranalli gratefully acknowledges the support of the Oak Ridge Institute for Science and Education (ORISE) Postdoctoral Fellowship program.

References

[1]Botero, C.; Finkenrath, M.; Bartlett, M.; Chu, R.; Choi, G.; Chinn, D. "Redesign, Optimization, and Economic Evaluation of a Natural Gas Combined Cycle with the Best Integrated Technology CO2 Capture," *Energy Procedia,* Vol. 1, 2009, pp. 3835-3842.

[2]Durox, D.; Schuller, T.; Candel, S. "Combustion dynamics of inverted conical flames," *Proceedings of the Combustion Institute,* Vol. 30, 2005, pp. 1717-1724.

[3]Ranalli, J.; Martin, C.; Black, P.; Vandsburger, U.; West, R. "Measurement of Flame Transfer Functions in Swirl-Stabilized, Lean-Premixed Combustion," *Journal of Propulsion and Power,* Vol. 25, 2009, pp. 1350-1354.

[4]Lohrmann, M.; Buchner, H. "Prediction of stability limits for LP and LPP gas turbine combustors," *Combustion Science and Technology,* Vol. 177, 2005, pp. 2243-2273.

[5]Balachandran, R.; Ayoola, B.; Kaminski, C.; Dowling, A.; Mastorakos, E. "Experimental investigation of the nonlinear response of turbulent premixed flames to imposed inlet velocity oscillations," *Combustion and Flame,* Vol. 143, 2005, *pp.* 37-55.

[6]Ducruix, S.; Durox, D.; Candel, S. "Theoretical and experimental determinations of the transfer function of a laminar premixed flame," *Proceedings of the Combustion Institute,* Vol. 28, 2000, pp. 765-773.

[7]Palies, P.; Durox, D.; Schuller, T.; Candel, S. "The combined dynamics of swirler and turbulent premixed swirling flames," *Combustion and Flame,* Vol. 157, 2010, pp. 1698-1717.

[8]Kim, K.; Lee, J.; Quay, B.; Santavicca, D. "Spatially distributed flame transfer functions for predicting combustion dynamics in lean premixed gas turbine combustors," *Combustion and Flame,* Vol. 157, 2010, pp. 1718-1730.

[9]Kim, D.; Park, S. W. "Effects of hydrogen addition on flame structure and forced flame response to velocity modulation in a turbulent lean premixed combustor," *Fuel*, Vol. 89, 2010, pp. 3475-3481.

[10]Külsheimer, C.; Büchner, H. "Combustion dynamics of turbulent swirling flames," *Combustion and Flame,* Vol. 131, 2002, pp. 70-84.

[11]Johnson, M.; Littlejohn, D.; Nazeer, W.; Smith, K.; Cheng, R. "A comparison of the flowfields and emissions of high-swirl injectors and low-swirl injectors for lean premixed gas turbines," *Proceedings of the Combustion Institute,* Vol. 30, 2005, pp. 2867-2874.

[12]Cheng, R.; Littlejohn, D.; Strakey, P.; Sidwell, T. "Laboratory investigations of a low-swirl injector with H2 and CH4 at gas turbine conditions," *Proceedings of the Combustion Institute,* Vol. 32, 2009, pp. 3001-3009.

[13]Kang, D.; Culick, F.; Ratner, A. "Combustion dynamics of a low-swirl combustor," *Combustion and Flame,* Vol. 151, 2007, pp. 412-425.

[14]Yilmaz, I.; Ratner, A.; Ilbas, M.; Huang, Y. "Experimental investigation of thermoacoustic coupling using blended hydrogen-methane fuels in a low swirl burner," *International Journal of Hydrogen Energy,* Vol. 35, 2010, pp. 329-336.

[15]Ferguson, D.; Ranalli, J.; Strakey, P. In *Proceedings of the ASME Turbo Expo*; Glasgow, UK, 2010; Vol. GT2010-23642.

[16]Preetham; Santosh, H.; Lieuwen, T. "Dynamics of Laminar Premixed Flames Forced by Harmonic Velocity Disturbances," *Journal of Propulsion and Power,* Vol. 24, 2008, pp. 1390-1402.

[17]You, D.; Huang, Y.; Yang, V. "A generalized model of acoustic response of turbulent premixed flame and its application to

gas-turbine combustion instability analysis," *Combustion Science and Technology,* Vol. 177, 2005, pp. 1109-1150.

[18]Kim, K. T.; Lee, J. G.; Lee, H. J.; Quay, B. D.; Santavicca, D. A. "Characterization of Forced Flame Response of Swirl-Stabilized Turbulent Lean-Premixed Flames in a Gas Turbine Combustor," *J. Eng. Gas Turbines Power,* Vol. 132, 2010, 041502-8.

[19]Lee, J.; Santavicca, D. "Experimental diagnostics for the study of combustion instabilities in lean premixed combustors," *Journal of Propulsion and Power,* Vol. 19, 2003, pp. 735-750.